CONF-840530--1

Talk given by J. Gizon at the International Symposium on In-Beam Nuclear Spectroscopy, Debrecen, Hungary, May 14-18, 1984.

CONF-840530--1

DE84 012327

DYNAMIC MOMENTS OF INERTIA IN Xe, Cs AND Ba NUCLEI

H. El-Samman, V. Barci, A. Gizon, J. Gizon, L. Hildingsson*
D. Jerrestam*, W. Klamra*, R. Kossakowski, Th. Lindblad*
Institut des Sciences Nucléaires (IN2P3), Grenoble, France

Y. Gono
The Institute of Physical and Chemical Research, Saitama, Japan

T. Bengtsson
Department of Mathematical Physics, Institute of Technology, Lund, Sweden

G.A. Leander
UNISOR, Oak Ridge, Tennessee, USA

The γ-rays following the reactions induced by ^{12}C ions on ^{115}In, $^{112,117,122}Sn$ and ^{123}Sb targets have been investigated using six NaI(Tl) detectors in a two-dimensional arrangement. The collective moment of inertia $\mathcal{J}^{(2)}_{band}$ of $^{118,122}Xe$, ^{123}Cs and $^{128,130}Ba$ have been excracted from the energy-correlation spectra. The behaviour of these nuclei and the observed differences are interpreted in terms of high-spin collective properties. Data are also presented on the effective moment of inertia $\mathcal{J}^{(2)}_{eff}$ of ^{118}Xe and ^{130}Ba measured by sum-spectrometer techniques.

1. INTRODUCTION

Informations on nuclear structure at high angular momentum can be obtained from studies of "discrete" and "unresolved" γ-ray spectra. The latter method is based on the detection of the γ-ray continuum and concerns essentially gross properties of the nuclei e.g. the determination of moments of inertia.

It is well known that the nuclei generate angular momentum by collective rotation of the nucleus as a whole as well as by particle alignment. The two kinds of behaviour can be evidenced by studies of dynamic moments of inertia $\mathcal{J}^{(2)} = \hbar(dI/d\omega)$ which describe the rate of change of spin with the rotational frequency. Thus,

- a collective moment of inertia $\mathcal{J}^{(2)}_{band} = \hbar(dI/d\omega)_{band}$ can be deduced for the bands generated by the collective motion. It is measured in γγ-energy correlation experiments.
- an effective moment of inertia $\mathcal{J}^{(2)}_{eff} = \hbar(dI/d\omega)_{path}$ is connected to the decay path along the envelope of these bands. It is related to both the collective motion and the alignment of particles. It may be measured by employing sum-spectrometer techniques to correct for feeding.

These two dynamic moments of inertia have been measured in several transitional nuclei of the 50 < Z,N < 82 region. Experimental results are reported here and comparisons are made with model calculations.

2. THE COLLECTIVE MOMENT OF INERTIA $\mathcal{J}^{(2)}_{band}$ OF Xe and Ba NUCLEI

For a perfect rotor having level energies proportional to I(I+1), the transition energies ($\Delta I = 2$) are equal to $E_\gamma = (4I-2)\hbar^2/2\mathcal{J}$. In a $\gamma\gamma$-coincidences experiment, this will generate a matrix of correlated events with no intensity along the diagonal $E_{\gamma 1} = E_{\gamma 2}$. The width of the central valley W which measures twice the difference in transition energies ΔE_γ is inversely proportional to the dynamical moment of inertia $\mathcal{J}^{(2)}_{band}$ i.e. $W = 2\Delta E_\gamma = 4\, dE_\gamma/dI = 8\, d^2E/dI^2 = 8\hbar^2/\mathcal{J}^{(2)}_{band}$ where E is the level excitation energy.

During the last few years several experiments have been performed in the Ba-Xe region [cf ref. 1,2 and references therein]. These investigations have revealed different behaviour of the collective moment of inertia $\mathcal{J}^{(2)}_{band}$ with the rotational frequency. In order to gain further knowledge on this behaviour, experiments were undertaken at the Grenoble cyclotron to study light Xe nuclei and heavier Ba nuclei. The results presented here are part of a publication [3].

2.1. Experimental techniques

Six NaI(Tl) detectors are used to record $\gamma\gamma$-coincidence spectra. They are 8" long and have a hexagonal cross-section with a 6" outer diameter. To prevent scattering, they are shielded with lead and their entrance window is collimated. They are placed at 25 cm from the target at an angle of 125° relative to the beam. Their solid angle is 0.27 % of 4π and their energy resolution is better than 8 % for the 661 keV γ-line of ^{137}Cs. A Ge(Li) detector, perpendicular to the beam axis, is used to identify the final reaction products.

Four enriched self-supporting targets of about 4 mg/cm^2 thickness are bombarded with ^{12}C ions from the Grenoble variable energy cyclotron. For each target, approximately 7×10^7 NaI(Tl) coincidence events are recorded. Since all events involving two or more detectors in coincidence are written on magnetic tapes to be subsequently analyzed into one single two-dimensional matrix, the gains of the amplifiers are carefully matched and monitored throughout the experiment.

In a separate experiment, the γ-ray multiplicities are determined for the ^{112}Sn and ^{122}Sn targets. They are deduced from the number of counters (12 NaI(Tl) crystals of a sum-spectrometer) triggered in coincidence with a Ge detector.

2.2. Experimental results

The coincidence data are sorted off-line into a two-dimensional matrix which is made symmetric with respect to the diagonal $E_{\gamma 1} = E_{\gamma 2}$. The Copenhagen subtraction scheme is applied in order to enhance the correlated photopeak-photopeak events.

In the present experiments, the moment of inertia $\mathcal{J}^{(2)}_{band}$ is obtained by measuring the distance between the peaks of the first ridge in cuts perpendicular to the diagonal.

Bridges accross the valley are typical for crossing between bands and can give informations on rotational alignment of particles. These bridges are indicated by triangles in figs. 1-4.

2.2.1. The $^{112}Sn + ^{12}C$ reaction at 112 MeV

The main final nuclei are ^{118}Xe and ^{116}Te which represent 38% and 28 % respectively, of the total intensity. In this experiment, the γ-multiplicities were measured but the results do not show a significant difference between ^{118}Xe and ^{116}Te. The reason for this is that many lines in the Ge(Li) spectra are doublets, i e. a mixture of transitions of the two final nuclei mentioned. However, one would expect the ^{116}Te nucleus to have a smaller value since it is formed following the emission of two more protons. This argument together with the relative intensities implies that the energy-energy correlation matrix in the $^{112}Sn + ^{12}C$ reaction is dominated by ^{118}Xe at high γ-ray energies.

The correlation matrix does not exhibit a well defined valley at lower energies. Furthermore, when the valley starts to develop at E_γ = 0.450 MeV, it is a valley with many "fillings" and bridges. This explains why there are only a few values of $\mathcal{J}^{(2)}_{band}$ determined up to $\hbar^2\omega^2$ = 0.08 MeV^2 (fig. 1). The strong bridge at E_γ = 0.775 MeV is due to the backbend in ^{118}Xe. The highest value (44 $\hbar^2$ MeV^{-1}) of $\mathcal{J}^{(2)}_{band}$ results in the narrowing of the valley due to the coincidence between the γ-rays deexciting the 12^+ and 8^+ levels in ^{118}Xe.

For frequencies higher than $\hbar^2\omega^2$ = 0.17 MeV^2, the moment of inertia $\mathcal{J}^{(2)}_{band}$ is almost constant and equals 30 $\hbar^2$ MeV^{-1} on both side of a filling in the valley at E_γ = 1.01 MeV ($\hbar^2\omega^2$ = 0.254 MeV^2). The valley terminates with a strong bridge at E_γ = 1.20 MeV.

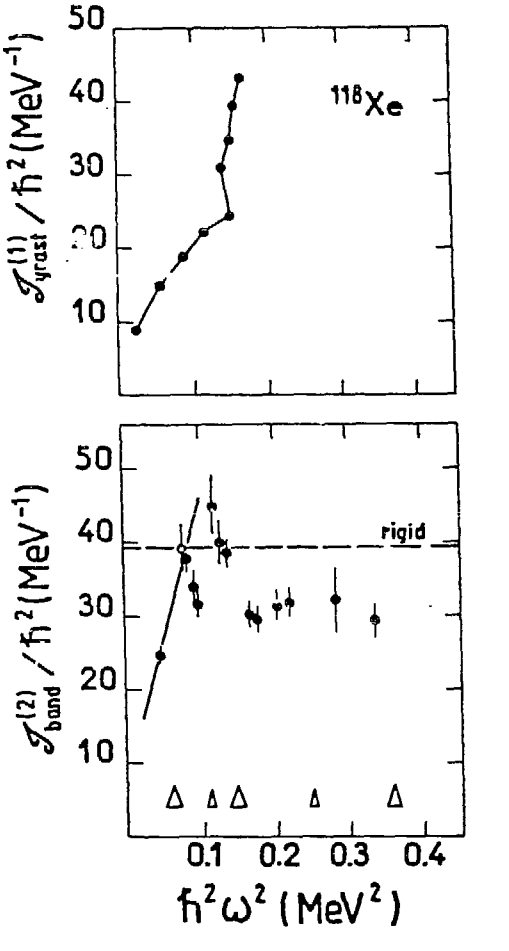

Fig 1 : The moments of inertia $\mathcal{J}^{(1)}$ and $\mathcal{J}^{(2)}$ as obtained from the discrete transitions and the correlation experiment respectively. The solid line in the lower part of the figure is the moment $\mathcal{J}^{(2)}_{yrast}$ deduced from the lowest discrete lines.

2.2.2. The ^{117}Sn + ^{12}C reaction at 118 MeV

The nuclei ^{123}Cs, $^{120-123}Xe$ and $^{118,121}Te$ are clearly identified in the singles and coincidences germanium spectra. From the ratios of γ-rays intensities in the spectrum of a Ge detector in coincidence with two or more NaI crystals to the singles, it appears that the Xenons and ^{123}Cs have approximately the same multiplicity which is much larger than that of the telluriums, as expected. Such a ratio is not enough precise to make a difference between the xenons and cesium but considering the intensities in the various channels ^{122}Xe dominates very likely in the high energy part of the correlation matrix.

The main bridge at E_γ = 0.79 MeV corresponds to the backbend in ^{122}Xe and ^{120}Xe. The dynamic moment of inertia $\mathcal{J}^{(2)}_{band}$ (fig. 2) which is equal to 34 $\hbar^2$ MeV^{-1} at its maximum drops to 25 $\hbar^2$ MeV^{-1} after the first backbend and remains almost constant up to $\hbar^2\omega^2$ = 0.46 MeV^2.

2.2.3. The ^{123}Sb + ^{12}C reaction at 118 MeV

The nucleus ^{128}Ba which represents more than 46 % of the total intensity should be the nucleus which mainly influences the energy-energy correlation matrix.

The variations of $\mathcal{J}^{(2)}_{band}$ in function of $\hbar^2\omega^2$ are plotted in the range 0.07 - 0.36 MeV^2 (fig. 3). The bridge at E_γ = 0.890 MeV corresponds exactly to the coincidence between the lines deexciting the 12^+ and 10^+ levels in ^{128}Ba. When going to higher frequencies, $\mathcal{J}^{(2)}_{band}$ increases up to the rigid body value (45 $\hbar^2$ MeV^{-1}) at $\hbar^2\omega^2$ = 0.32 MeV^2. One must point out the existence of a bridge at 1.040 MeV and the very low value (32.5 $\hbar^2$ MeV^{-1}) at $\hbar^2\omega^2$ = 0.255 MeV^2 which constitutes a dip in the $\mathcal{J}^{(2)}_{band}$ curve (fig. 3).

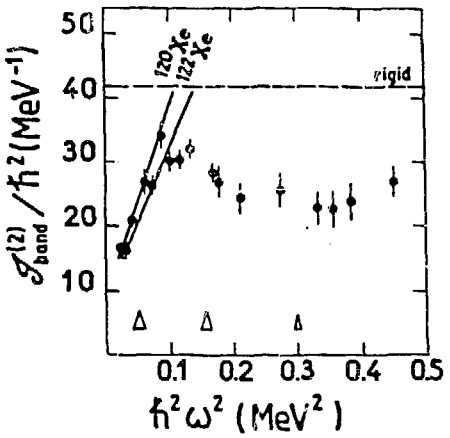

Fig.2 : The collective moment of inertia of ^{122}Xe.

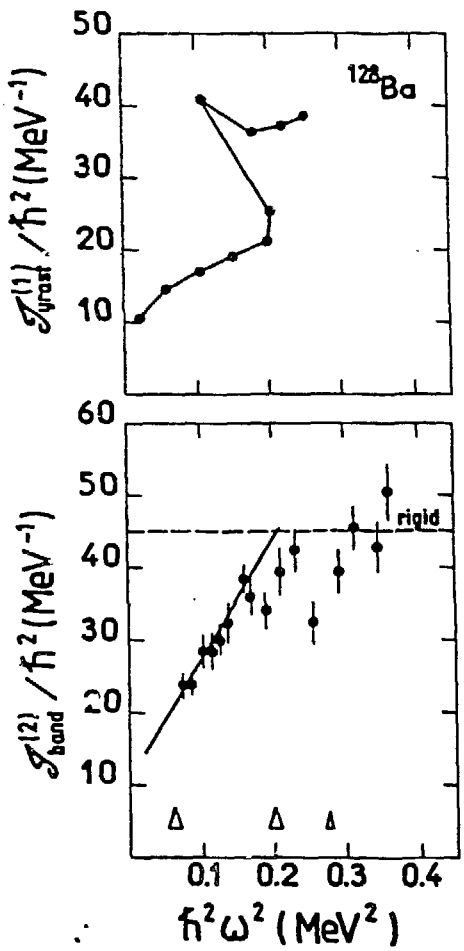

Fig.3 : The collective moment of inertia of ^{128}Ba.

2.2.4. The $^{122}Sn + ^{12}C$ reaction at 80 MeV

The yrast cascade of ^{130}Ba is the most strongly fed in this reaction. From the γ-multiplicity measurements, it is clear that its γ-lines are associated with the largest prompt multiplicity. Therefore, ^{130}Ba is the preponderant nucleus in the correlation matrix.

A very clear valley appears in the matrix up to 1.14 MeV γ-ray energy. The width decreases continuously and there is no apparent bridge between $E_\gamma = 0.400$ and 1.095 MeV. However a hill in the bottom of the valley shows up at $E_\gamma = 0.760$ MeV in a cut made along the main diagonal. It is due to coincidences between the γ-lines depopulating the 14^+ and 12^+ levels in the backbending region of ^{130}Ba. It may be noted (fig. 4) that after this backbend, $\mathcal{J}^{(2)}_{band}$ increases very slightly up to approximately 90 % of the rigid rotor value (46 $\hbar^2$ MeV^{-1}) near the strong bridge which terminates the valley at $E_\gamma = 1.095$ MeV.

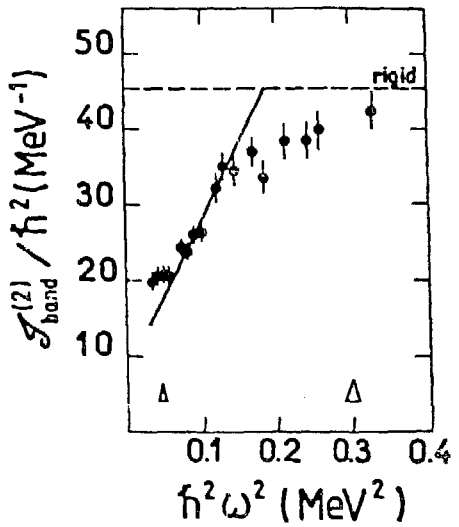

Fig. 4 : The collective moment of inertia of ^{130}Ba.

2.3. Discussion of the dynamic moment of inertia $\mathcal{J}^{(2)}_{band}$

The collective moment of inertia of the ground band which is related to the discrete γ-ray transitions by the formula $\mathcal{J}^{(1)} \equiv (4I-2)\hbar/4\omega$ can be parametrized within the VMI model i.e. $\mathcal{J}^{(1)}_{yrast}(\omega) = \hbar I/\omega = \mathcal{J}_0 + \mathcal{J}_1\omega^2$ where $\mathcal{J}_0$ and $\mathcal{J}_1$ are two parameters.

Before the first backbend, the dynamic moment of inertia $\mathcal{J}^{(2)}_{band}$ which is deduced from the width of the valley in a correlation matrix and is proportional to the first derivative $dI/d\omega$ can be compared to $\mathcal{J}^{(2)}_{yrast} = \mathcal{J}_0 + 3\mathcal{J}_1\omega^2$ (straight lines in figs. 1-4,6) obtained from the preceding equation. Generally the two $\mathcal{J}^{(2)}$ values agree quite well.

2.3.1. The xenon nuclei

As a general remark, one sees from the $\mathcal{J}^{(2)}_{band}(\omega^2)$ curves that both the above defined moments of inertia $\mathcal{J}^{(2)}_{band}$ and $\mathcal{J}^{(2)}_{yrast}$ agree well up to the frequencies of the first backbend. In fig. 2, one notices that the measured values of $\mathcal{J}^{(2)}_{band}$ are separated in two sets, both fitting the straight lines $\mathcal{J}_0 + 3\mathcal{J}_1\omega^2$ corresponding to ^{120}Xe and ^{122}Xe. This is explained by the intense γ-rays deexciting the first levels of these two isotopes.

$\mathcal{J}^{(2)}_{band}$ of both $^{118,122}Xe$ behave in a similar way i.e. decrease strongly after the first backbend down to roughly two thirds of the rigid sphere value (figs. 1,2). The first backbending in $^{124,126,128,130}Xe$ originates from the coupling of two $h_{11/2}$ neutrons [4]. For the lighter isotopes, the situation is more uncertain. However, calculations made with the Bengtsson and Frauendorf model [5] indicate that band crossings of $h_{11/2}$ protons and neutrons can occur at nearby frequencies, the latter being more probable.

Our data on ^{118}Xe enlarge towards lighter masses and more neutron-deficient nuclei previous measurements made on xenon isotopes [1,2]. Our results

on ^{122}Xe extend to higher frequencies (up to $\hbar\omega$ = 0.67 MeV) the data already known from the ^{116}Sn + ^{12}C reaction [1].

2.3.2. The barium nuclei

As in the xenons, the experimental $\mathcal{J}^{(2)}_{band}$ values, can be fitted with a $\mathcal{J}_0 + 3\,\mathcal{J}_1\omega^2$ polynomial below the firs particle alignment.

The variations of $\mathcal{J}^{(2)}_{band}$ in both ^{128,130}Ba look very similar (figs.3,4) except for the reduction in ^{128}Ba at $\hbar^2\omega^2$ = 0.255 MeV^2 i.e. immediately after the backbend. We show in fig. 4, that this dip has disappeared in ^{130}Ba or almost entirely disappeared if one takes into account the very shallow minimum at $\hbar^2\omega^2$ = 0.185 MeV^2. This could mean that the collective moment of inertia is less affected by particle alignment in ^{130}Ba than in ^{126,128}Ba.

Two band crossings have been found in ^{128}Ba, [ref.6] and ^{130}Ba [ref.7]. Alignment considerations and cranking model calculations both predict a $h_{11/2}$ neutron origin for the lowest one in ^{130}Ba while the second is generated by $h_{11/2}$ protons [7]. A backbend has been discovered in ^{130}Ce [ref.8] at high frequency ($\hbar\omega$ = 0.58 MeV). This third backbend (after the $\pi h_{11/2}$ and $\nu h_{11/2}$ alignments) is expected from $i_{13/2}$ neutrons. If the isotones behave the same way, ^{128}Ba should also exhibit such a high frequency alignment. We propose that the bridge observed at $\hbar\omega$ = 0.52 MeV in the ^{128}Ba correlation matrix could proceed from $i_{13/2}$ neutrons as the one found at $\hbar\omega$ = 0.55 MeV in ^{130}Ba.

2.3.3. The difference between the Ba and Xe nuclei

The moment of inertia of the Xe decreases after the first band crossing and remains small and almost constant at high frequency while it increases in the latter all along with the frequency. Such a qualitative difference in the quasicontinuum data could reflect changes in the high-spin collective properties, particularly the shape, with changing nucleon number.

For a possible interpretation of the results we can look to high-spin potential energy of deformation surfaces, which have been calculated for these nuclei by the cranked Nilsson-Strutinsky method [9]. A recent study [10] which also included pairing has clarified systematic trends of microscopic origin which are manifested by the numerical results : the alignment of high-j quasiparticle orbitals drives the nuclear shape toward regions of collective or non-collective rotation, depending on the position of the Fermi levels in the j-shell. The valence shells of light xenon and barium isotopes include the neutron and proton $h_{11/2}$ intruder shells. The general systematics of reference [10] would suggest a more collective behaviour in the bariums than the xenons after initial quasiparticle alignment, considering the position of the Fermi level in these shells. We have carried out calculations using the method of reference [11] where individual bands are constructed and traced up to high spins. Table 1 and fig. 5 show the results for the nuclei ^{122}Xe and ^{128}Ba.

In ^{122}Xe, we find three different kinds of states near yrast (c.f.table 1). There are collective prolate bands at $\gamma \simeq 0$ with $\mathcal{J}^{(2)}_{band} \gtrsim 35\ \hbar^2$ MeV^{-1}, moderately collective triaxial bands at $\gamma \simeq 30°$ with $\mathcal{J}^{(2)}_{band} < 30\ \hbar^2$ MeV^{-1}, and non-collective states of particle-hole character at $\gamma \simeq 60°$. The data can be taken to indicate that it is the $\gamma \simeq 30°$ triaxial bands which come lowest in energy and dominate the γ cascade in ^{122}Xe. The observed features in ^{122}Xe fit the description of the moderately collective, $\gamma \simeq 30°$ triaxial bands.

Table 1 : Moment of inertia $\mathcal{J}^{(2)}_{band}$ for bands in ^{122}Xe and in ^{128}Ba. The first column shows the most important part of the configuration. Letters (A)-(E) refer to the bands in fig. 5.

^{122}Xe Configuration	ε	γ	range I	range $\hbar\omega$ (MeV)	$\mathcal{J}^{(2)}_{band}$ $\hbar^2$MeV^{-1}
$\pi(h_{11/2})^1\nu(h_{11/2})^6$	0.28	0°	6-24	-0.5	∿ 36
$\pi(h_{11/2})^1\nu(h_{11/2})^6$	0.24	33°	6-20	-0.5	∿ 28
$\pi(h_{11/2})^2\nu(h_{11/2})^6$	0.28	0°	10-36	0.1-0.7	∿ 38
$\pi(h_{11/2})^2\nu(h_{11/2})^6$	0.25	33°	18-26	0.3-0.5	∿ 30

^{128}Ba Configuration	ε	γ	range I	range $\hbar\omega$ (MeV)	$\mathcal{J}^{(2)}_{band}$ $\hbar^2$MeV^{-1}
$\pi(h_{11/2})^2\nu(h_{11/2})^8$	0.24	-50°	4-30	-0.6	∿ 34 (A)
$\pi(h_{11/2})^2\nu(h_{11/2})^8$	0.18	5°	24-38	0.5-0.8	∿ 34 (B)
$\pi(h_{11/2})^2\nu(h_{9/2})^2$	0.34	0°	16-36	0.2-0.8	∿ 35 (C)
$\pi(h_{11/2})^3\nu(h_{9/2})^2$	0.34	0°	22-44	0.4-1.0	∿ 38 (D)
$\pi(h_{11/2})^3\nu[(h_{9/2})^2 i_{13/2}]$	0.34	0°	30-	0.4-	∿ 40 (E)

For ^{128}Ba, the calculated near-yrast levels are collective with $\mathcal{J}^{(2)}_{band} > 30\ \hbar^2\ MeV^{-1}$. A further mechanism for the continued increase of $\mathcal{J}^{(2)}_{band}$ at high spins in ^{128,130}Ba, but not ^{118,122}Xe, is provided by a secondary minimum at larger deformation in the potential-energy surfaces [9]. This minimum at ε ∿ 0.34, γ ∿ 0° corresponds to bands with a pair of aligned $h_{9/2}$ neutrons. With additional $i_{13/2}$ neutron alignment such bands may cross the valence bands and become yrast at very high spins [11]. The energy of the strongly deformed (ε ∿ 0.34) potential energy minimum relative to the valence shell (ε ∿ 0.24) minimum decreases for increasing proton and neutron number up to an optimum of about Z = 60 and N = 72, [ref. 9]. For the barium isotopes (Z = 56, N = 72, 74) these bands

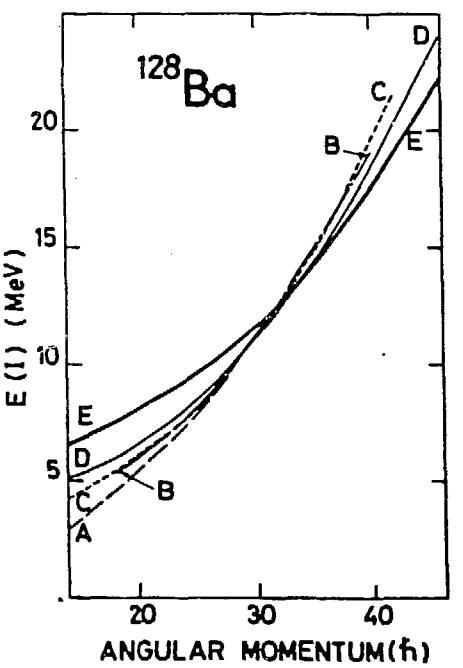

Fig.5 : Calculated bands in ^{128}Ba.

are not expected to be yrast at the very highest spins reached in the present experiment. Nevertheless, over a wide range of lower spins they are likely to retain a significant fraction of the total population from a (HI, ypxn) reaction. These strongly collective bands would then dominate the $E_\gamma - E_\gamma$ correlations and account for the larger $\mathcal{J}^{(2)}_{band}$ values in the barium isotopes.

3. $\mathcal{J}^{(2)}_{band}$ IN ^{123}Cs AND INFLUENCE OF A PROTON

As developed previously, there is a great difference in the behaviour of the xenons and bariums. Since both the numbers of protons and neutrons differ in these Xe and Ba isotopes, we have tried to limit the variations to only one of these numbers in order to separate the characteristic influence of protons or neutrons. We have performed an experiment to measure the collective moment of inertia of ^{123}Cs which can be considered as a ^{122}Xe core plus a proton.

3.1. The experiment

We have used the apparatus and techniques described in section 2. The reaction was ^{115}In + ^{12}C at 80 MeV with a 6 mg/cm^2 target, enriched to 99.8%. About 1.3 x 10^8 prompt in-beam $\gamma\gamma$-coincidence events were recorded.

The cross-section of the 4n channel is the most intense. ^{123}Cs which represents 56 % of the total intensity and has the largest multiplicity, dominates in the correlation matrix.

A central valley shows up in this matrix. The known γ-rays which deexcite the $h_{11/2}$ cascade [12] define the ridges in the low energy part. Then, the valley continues up to its end-point at E_γ = 1.25 MeV.

3.2. Discussion of the cesium behaviour

In fig. 6 where $\mathcal{J}^{(2)}_{band}$ of ^{123}Cs and ^{122}Xe are plotted as a function of $\hbar^2\omega^2$, one observes that :

i) up to $\hbar^2\omega^2 \simeq 0.15$ MeV^2, the collective moment of inertia of ^{123}Cs follows the $\mathcal{J}_0 + 3\mathcal{J}_1\omega^2$ relationship in the VMI model, as indicated by the solid straight line

ii) in the range $\hbar^2\omega^2 \simeq 0.15 - 0.32$ MeV^2, $\mathcal{J}^{(2)}_{band}$ has the same trends in ^{123}Cs and ^{122}Xe i.e. decreases and then, stays almost constant around $25\hbar^2$ MeV^{-1}.

iii) above $\hbar^2\omega^2 \gtrsim 0.32$ MeV^2, the moment of inertia of ^{123}Cs increases rapidly to the rigid sphere value while it remains constant in ^{122}Xe.

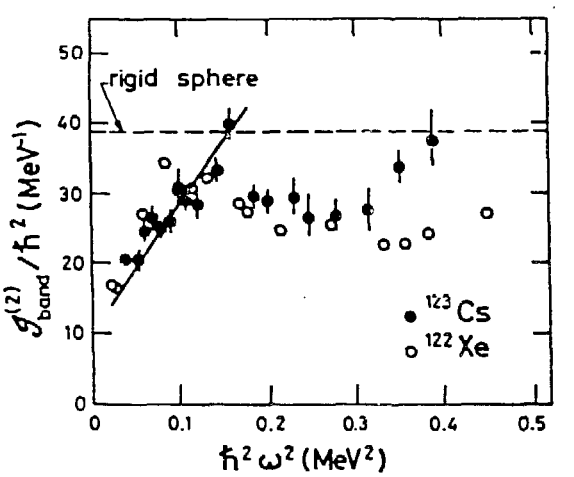

Fig.6 : The collective moment of inertia of ^{123}Cs.

The difference in the amplitude of $\mathcal{J}^{(2)}_{band}$ for ^{123}Cs and ^{122}Xe observed at high frequency concerns the continuum data related to the high spin collective properties and could result in the addition of a proton to the xenon core.

The method of tracing states up to high spins [11] which was successfully applied to the Xe and Ba isotopes (see section 2.3.3.) has been also used to compare the nuclear structure of ^{123}Cs and ^{122}Xe. The configurations of the xenon for which the moment of inertia was calculated (table 1), have also been analyzed in the cesium. It appears that the $\pi(h_{11/2})^2\ \nu(h_{11/2})^6$ band in ^{123}Cs with a prolate deformation ($\gamma \simeq 0°$) is lower than the band with the same configuration at $\gamma \simeq 30°$ above spin 20 $\hbar$. The moment of inertia corresponding to the prolate shape equals 35-40 $\hbar^2$ MeV^{-1} while it is only 30 $\hbar^2$ MeV^{-1} in ^{122}Xe. The experimental results on the xenons (section 2.) indicate that ^{122}Xe tends to favour the triaxial band.

Therefore it is tempting to interpret the rise of $\mathcal{J}^{(2)}_{band}$ in ^{123}Cs as a change of deformation from $\gamma \simeq 30°$ to $\gamma \simeq 0°$.

4. THE EFFECTIVE MOMENT OF INERTIA $\mathcal{J}^{(2)}_{eff}$

The decay path of a nucleus may consist of many rotational bands which can have different alignments. Thus, the effective moment of inertia $\mathcal{J}^{(2)}_{eff} = \hbar\ (dI/d\omega)_{path}$ related to the envelope of these bands includes both the collective motion of the nucleus and the alignment of particles. Experiments have been already made to measure this dynamic moment of inertia in well deformed nuclei of the rare earth region i.e. Er and Yb isotopes [13]. We report here on such measurements for transitional nuclei.

4.1. The experimental set-up and techniques

The physical information is extracted from continuum γ-ray spectra delivered by a big NaI(Tl) detector (8" long and a hexagonal cross-section with 6" outer diameter) in coincidence with a sum-spectrometer. The former detector is placed at 125° to the beam direction and its entrance window is strongly collimated. The sum-spectrometer is made of 12 such hexagonal detectors arranged in a cylindrical geometry with the symmetry axis coinciding with the beam. Since this sum-spectrometer consists of 12 detectors, the γ-ray multiplicity is evidently deduced from a fit of the experimental fold-distribution. A Ge(Li) counter is used in order to identify the final nuclei.

The technique to deduce the effective moment of inertia is the following. First, the raw spectra of the lonely NaI crystal in coincidence with slices of the total γ-ray energy are unfolded. Then, the unfolded spectra are normalized to the multiplicity and the statistical component $E_\gamma^3 \exp(-E_\gamma/T)$ is subtracted. The last step consists in a feeding correction [13] to take into account the different populations of the states.

4.2. Analysis of the results

We measured the effective moment of inertia of ^{116}Xe and ^{130}Ba which were previously studied by the correlation technique to give the collective moment of inertia $\mathcal{J}^{(2)}_{band}$ (section 2.).

The results are shown in figs. 7 and 8 for the $\hbar\omega$ = 0.2 - 0.7 MeV range (full solid line). The bumps are associated with intense γ-lines between the lowest levels of yrast-cascade and with an accumulation of γ-rays due to particle alignment.

For ^{118}Xe (fig. 7), the peak at $\hbar\omega$ = 0.39 MeV corresponds to the backbend. Its frequency matches perfectly with the one of a bridge in the $\gamma\gamma$-correlation matrix ($h_{11/2}$ protons and neutrons). The bumps at 0.52 and 0.62 MeV also fit with bridges in the correlation plots, but the nature of the particles which align their angular momentum is still unknown.

In the ^{130}Ba case (fig.8), the peaks showing up at 0.27 and 0.34 MeV correspond to the $4^+ \rightarrow 2^+$ and $6^+ \rightarrow 4^+$ γ-rays. The bump at 0.40 MeV contains the two first band crossing originating from $h_{11/2}$ neutrons and protons [7]. By comparison with the correlation data, the broad peak around 0.53 MeV could be assigned to the $i_{13/2}$ neutrons alignment.

The theoretical moment of inertia can be deduced from the bands calculated within the cranked Nilsson-Strutinsky framework [11]. Up to now, only preliminary results are available. Thus, it is difficult to draw conclusions on the structure of the Xe and Ba only considering $\mathcal{J}^{(2)}_{eff}$. However, these preliminary calculations agree with a qualitative comparison of $\mathcal{J}^{(2)}_{band}$ and $\mathcal{J}^{(2)}_{eff}$ which shows that ^{130}Ba is more collective than ^{118}Xe. Indeed, up to about $\hbar\omega \simeq 0.5$ MeV, the ratio $\mathcal{J}^{(2)}_{band} / \mathcal{J}^{(2)}_{eff}$ is larger in ^{130}Ba than in ^{118}Xe. This comes directly from the relation $\Delta i/\Delta I = 1 - \mathcal{J}^{(2)}_{band} / \mathcal{J}^{(2)}_{eff}$ where Δi is the increase in angular momentum due to particle alignment only and ΔI the total increase.

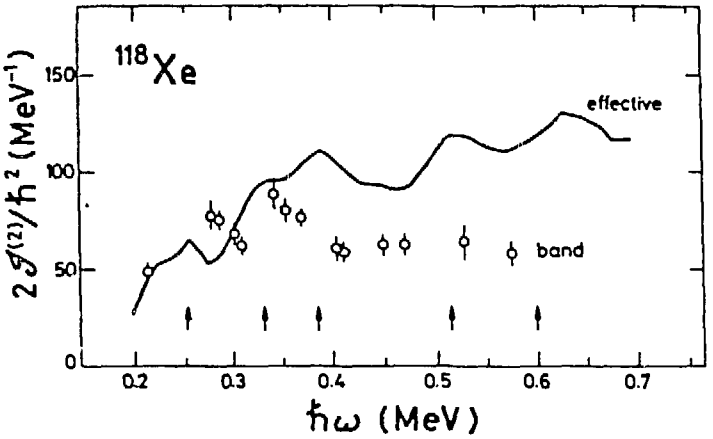

Fig.7 : The effective and collective moments of inertia of ^{118}Xe.

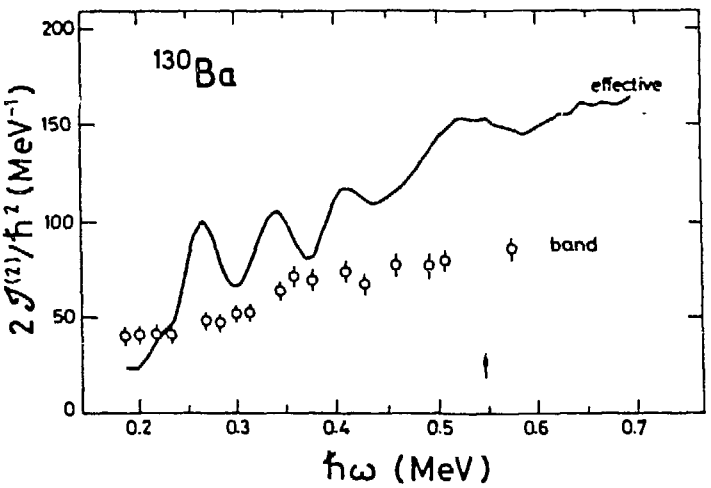

Fig.8 : The effective and collective moments of inertia of ^{130}Ba.

5. CONCLUSION

Results have been obtained on properties of transition nuclei at high spins. Collective and effective moments of inertia of Xe, Cs and Ba isotopes have been measured using γγ-correlation and sum-spectrometer techniques, respectively. The experimental data have been compared to model calculations. As a main conclusion, it appears that ^{128,130}Ba are more collective than ^{118,122}Xe.

This work was supported in part by Centre National de la Recherche Scientifique, by the Swedish Research Council for Natural Sciences (U-FR-8219-114) and by UNISOR, a consortium of 12 institutions, supported by them

and by the Office of Energy Research of the U.S.D.O.E. under contract DE-AC05 76OR00033 with Oak Ridge Associated Universities.

References

[1] Th. Lindblad, L. Hildingsson, D. Jerrestam, A. Källberg, A. Johnson, C.J. Herrlander, W. Klamra, A. Kerek, C.G. Linden, J. Kownacki, J. Bialkowski and T. Vertse, Nucl. Phys., A378 (1982) 364
[2] W. Klamra, J. Bialkowski, C.J. Herrlander, L. Hildingsson, D. Jerrestam, A. Johnson, A. Kerek, J. Kownacki, A. Källberg, Th. Lindblad, C.G. Linden, and T. Vertse, Nucl. Phys., A391 (1982) 184
[3] H. El-Samman, V. Barci, A. Gizon, J. Gizon, L. Hildingsson, D. Jerrestam, W. Klamra, R. Kossakowski, Th. Lindblad, T. Bengtsson and G.A. Leander, Nucl. Phys. to be published
[4] H. Hanewinkel, W. Gast, U. Kamp, H. Harter, A. Dewald, A. Gelberg, R. Reinhardt, P. Von Brentano, A. Zemel, C.E. Alonso and J.M. Arias, Phys. Lett., 133B (1983) 9
[5] R. Bengtsson and S. Frauendorf, Nucl. Phys., A327 (1979) 139
[6] K. Schiffer, A. Dewald, A. Gelberg, R. Reinhardt, K.O. Zell, P. Von Brentano and Sun Xiangfu, Z. Phys. A313 (1983) 245
[7] Sun Xianfgu, D. Bazzacco, W. Gast, A. Gelberg, U. Kamp, A. Dewald, K.O. Zell and P. Von Brentano, Phys. Rev. C28 (1983) 1167
[8] P.J. Nolan, R. Aryaeinejad, A.H. Nelson, D.J.G. Love, D.M. Todd and P.J. Twin, Phys. Lett. 128B (1983) 285
[9] S. Åberg, Phys. Scripta, 25 (1982) 23
[10] G.A. Leander, F. May and S. Frauendorf, in "High Angular Momentum Properties of Nuclei", ed. N.R. Johnson (Harwood, New York, 1983) p. 281
[11] T. Bengtsson and I. Ragnarsson, Phys. Lett., 115B (1982) 431
[12] N. Yoshikawa, J. Gizon and A. Gizon, J. Phys. Lett. 39 (1978) L-102
[13] M.A. Deleplanque, H.J. Körner, H. Kluge, A.O. Macchiavelli, N. Bendjaballah, R.M. Diamond and F.S. Stephens, Phys. Rev. Lett. 50 (1983) 409